Type synthesis of variable-DOF single-loop spatial mechanisms using Bennett 4R mechanisms and Goldberg 5R mechanisms

Digital Object Identifier (DOI):
10.1016/j.mechmachtheory.2024.105902

Mechanism and Machine Theory 206 (2025) 105902

Contents lists available at ScienceDirect

Mechanism and Machine Theory

journal homepage: www.elsevier.com/locate/mechmt

Research paper

Type synthesis of variable-DOF single-loop spatial mechanisms using Bennett 4R mechanisms and Goldberg 5R mechanisms

Xianwen Kong

School of Engineering and Physical Sciences, Heriot-Watt University, Edinburgh, EH14 4AS, UK

ARTICLE INFO

Keywords:
Type synthesis
Variable-DOF mechanism
Construction approach
Overconstrained mechanism
Bennett 4R mechanism
Goldberg 5R mechanism
Screw theory

ABSTRACT

This paper deals with the type synthesis of variable-DOF (degree-of-freedom) single-loop spatial mechanisms — a class of reconfigurable mechanisms that DOF may change. A construction method is proposed to the type synthesis of variable-DOF single-loop mechanisms using Bennett 4R mechanisms and Goldberg 5R mechanisms. Using this approach, variable-DOF single-loop mechanisms can be obtained by first constructing multi-DOF multi-loop overconstrained mechanisms and then obtaining multi-DOF single-loop overconstrained mechanisms from these multi-DOF multi-loop mechanisms. Six types of variable-DOF single-loop 7R mechanisms and three types of variable-DOF single-loop 8R mechanisms have been obtained. No variable-DOF single-loop nR (n>8) mechanisms can be constructed using Bennett 4R mechanisms and Goldberg 5R mechanisms. Isomeric variations of these variable-DOF mechanisms can be further obtained by isomerization. This work provides a solid foundation for further investigation on variable-DOF single-loop mechanisms.

1. Introduction

Variable-DOF (degree-of-freedom) single-loop spatial mechanisms [1,2] (also called kinematotropic mechanisms [3,4] or kinematotropic metamorphic mechanisms [5]) are a class of reconfigurable mechanisms that can be reconfigured without disassembly. Significant progresses have been made in the type synthesis of such mechanisms [1–3,6–14]. Several approaches have been proposed to the type synthesis of variable-DOF single-loop spatial mechanisms, such as the construction methods [1,2,9,11–13], methods based on displacement group theory [3], intersection of surfaces [10], factorization of polynomials [8,14], or in-depth kinematic analysis [7], and origami-inspired method [5]. However, the types of variable-DOF single-loop spatial mechanisms are still very limited.

In [2], a variable-DOF single-loop 7R mechanism was constructed using two Bennett 4R mechanisms. A variable-DOF single-loop 8R mechanism that has a 3-DOF double-Bennett mode was proposed using different approaches in [5,8]. In [15,16], 1-DOF single-loop overconstrained 6R mechanisms were constructed using Bennett mechanisms. A number of 1-DOF two-mode single-loop mechanisms have been constructed using overconstrained 4-link and/or 5 link mechanisms in [17]. Based on the above work, this paper is to propose a systematic construction method for the type synthesis of variable-DOF single-loop spatial mechanisms using Bennett 4R mechanisms and Goldberg 5R Mechanisms. Multi-mode mechanisms involving two pairs of co-axial joints such as those in [7–9,18,19] are excluded from the type synthesis in this paper.

In Section 2, a construction approach to the type synthesis of variable-DOF single-loop spatial mechanisms using Bennett 4R mechanisms and Goldberg 5R mechanisms is proposed. Construction of variable-DOF single-loop spatial mechanisms and the isometric variations of these mechanisms are presented in Section 3. Finally, conclusions are drawn in Section 4.

E-mail address: X.Kong@hw.ac.uk.

https://doi.org/10.1016/j.mechmachtheory.2024.105902
Received 8 October 2024; Received in revised form 9 December 2024; Accepted 23 December 2024

Available online 8 January 2025

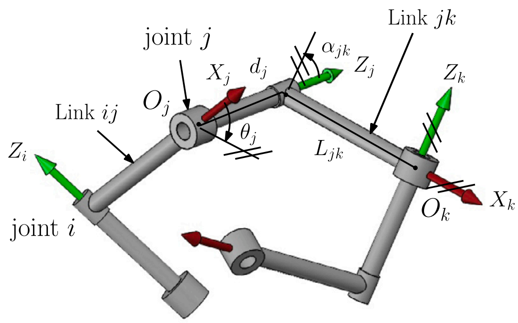

Fig. 1. Link parameters.

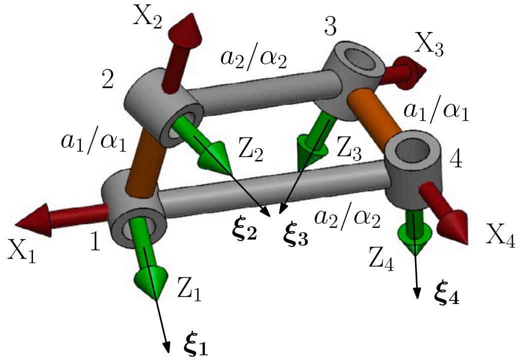

Fig. 2. Bennett 4R mechanism.

Throughout this paper, joints in a mechanism are numbered by 1, 2, ⋯, m, where m is the number of joints in the mechanism. A link is denoted by the joint numbers of all the joints on the link connected by "-". For example, link i-j refers to a link with joints i and j. Since the number of joints within a mechanism in this paper is no more than 9, "-" will be omitted for brevity. For example, the link with joints i and j is denoted by link ij, and link ijk refers to the ternary link with joints i, j and k. To facilitate the construction of variable-DOF mechanisms, ternary link ijk is regarded to be composed of three binary sub-links ij, jk, and ki. The frame of a mechanism is not indicated in the figures for simplicity.

Fig. 1 shows a kinematic sub-chain composed of three consecutive joints, i, j and k, of a mechanism. Following the original Denavit–Hartenberg convention,[1] the coordinate frames are attached to the links as follows: Z_i-, Z_j- and Z_k-axes are along the axes of joints i, j and k. X_j-axis is along the common perpendicular between Z_i- and Z_j-axes, X_k-axis is along the common perpendicular between Z_j- and Z_k-axes. The D-H (Denavit–Hartenberg) link parameters of link jk are defined as: θ_j (the joint angle between X_j- and X_k-axes measured from X_j-axis to X_k-axis about Z_j-axis), d_j (the distance between X_j- and X_k-axes measured from X_j-axis to X_k-axis along Z_j-axis), α_{jk} (the twist angle between Z_j- and Z_k-axes measured from Z_j-axis to Z_k-axis about X_k-axis), and L_{jk} (the distance between Z_j- and Z_k-axes measured from Z_j-axis to Z_k-axis along X_k-axis). The Bennett ratio of link jk is denoted by $B_{jk} = L_{jk}/\sin\alpha_{jk}$.

Overconstrained mechanisms or variable-DOF mechanisms may have links with the same link length and twist angle and/or links with the same absolute value of Bennett ratio. For example, one classic overconstrained mechanism, Bennett 4R mechanism (Fig. 2), has one DOF. The link parameters of the Bennett 4R mechanism 1-2-3-4-1 meet the following conditions:

$$\begin{cases} L_{12} = L_{34} \\ \alpha_{12} = \alpha_{34} \\ L_{23} = L_{41} \\ \alpha_{23} = \alpha_{41} \\ B_{12} = \pm B_{23} \\ d_i = 0 \quad i = 1,2,3,4 \end{cases} \tag{1}$$

[1] Link numbers are different from the original D-H convention to facilitate the description of multi-loop mechanisms. For a comparison of several D-H conventions, including the original, the distal variant, and the proximal variant, please refer to Ref. [20].

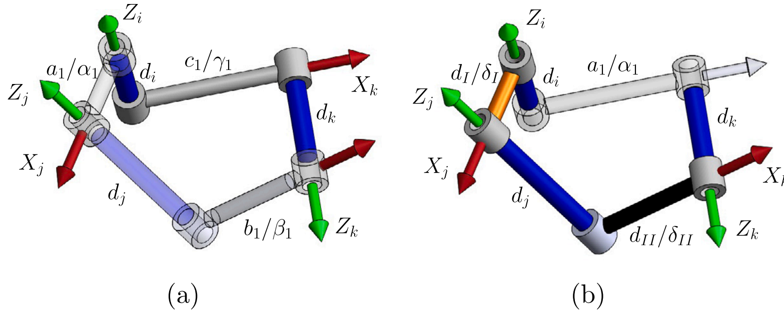

Fig. 3. (a) Replacement of two consecutive links ij and jk with link ik; and (b) Replacement of link ik with two consecutive links ij and jk.

To clearly represent the relations between these links in a figure, we introduce a_i/α_i ($i = 1, 2, 3, 4$), b_i/β_i ($i = 1, 2$), and c_i/γ_i (i=1, 2) to represent three groups of links with the same absolute value of Bennett ratio within each group. Here a_i, b_i and c_i represent the link lengths, and α_i, β_i and γ_i the twist angles of links. Links with the same link length and twist angle of a mechanism are also represented in the same color in the figures.

In the construction of overconstrained mechanisms and reconfigurable mechanisms, we also need to replace two consecutive links ij and jk with link ik (Fig. 3(a)) or vice versa (Fig. 3(b)). c_1/γ_1 is used to represent the length and twist angle of link ik in the former case as link combination while d_I/δ_I and d_{II}/δ_{II} are used to represent the lengths and twist angles of links ij and jk respectively in the latter case as link decomposition in the figures. The relations between the link parameters of these links have been well-documented in literature on spatial triangles such as [21].

2. Construction approach to the type synthesis of variable-DOF single-loop spatial mechanisms using Bennett 4R mechanisms and Goldberg 5R mechanisms

2.1. Mobility analysis of single-loop mechanisms

The formulas of instantaneous DOF, $\mathcal{F}$, of single-loop mechanisms are well-documented in the literature (see [22–27] for example). One formula for calculating the instantaneous $\mathcal{F}$ of a single-loop mechanism is (see [22] for example)[2]

$$\mathcal{F} = f - C \tag{2}$$

where f and C denote, respectively, the sum of the DOF of the joints and the order of the twist system composed of all the joint twists.

Rewriting Eq. (2), we can obtain C of a single-loop mechanism if the DOF, $\mathcal{F}$, of the mechanism is known as

$$C = f - \mathcal{F} \tag{3}$$

Let us take the 1-DOF Bennett 4R mechanism 1-2-3-4-1 (Fig. 2) as an example. Let ξ_i denote the unit twist along the joint axis of joint i of the Bennett 4R mechanism. Using Eq. (3), we obtain that the twist system of the Bennett 4R mechanism, which is composed of ξ_i (i=1, 2, 3, 4), is of order 3 ($C = f - \mathcal{F} = 4 - 1$). The basis of the twist system of the Bennett 4R mechanism can be represented by any three of ξ_i (i=1, 2, 3, 4), such as (ξ_1, ξ_2, ξ_3).

Now let us calculate the DOF of the single-loop 6R mechanism 1-2-3-4-5-6-1 shown in Fig. 4(a), which is obtained from the 2-loop mechanism composed of two Bennett 4R mechanisms 1-2-5-6-1 and 2-3-4-5-2 (Fig. 4(b)). Since the DOF of a Bennett 4R mechanism is 1, the DOF of the 2-loop mechanism (Fig. 4(b)) is 2. Since the single-loop 6R mechanism (Fig. 4(a)) is obtained from the 2-loop mechanism (Fig. 4(b)) by removing link 25, the DOF of the single-loop 6R mechanism (Fig. 4(a)) must be greater than or equal to 2 (the DOF of the 2-loop mechanism (Fig. 4(b)).

In the following, we will prove that the (full-cycle) DOF of the single-loop 6R mechanism (Fig. 4(a)) is 2 by further showing that the instantaneous DOF of the single-loop 6R mechanism is 2. The bases of the twist systems of the Bennett 4R mechanisms 1-2-5-6-1 and 2-3-4-5-2 can be represented by (ξ_1, ξ_2, ξ_5) and (ξ_2, ξ_3, ξ_5) respectively. The intersection of the twist systems of the two Bennett 4R mechanisms, the basis of which can be represented by (ξ_2, ξ_5), is of order 2. The twist system composed of the twists of all the six joints in the single-loop 6R mechanism (Fig. 4(a)) can be regarded as a linear combination of the twist system of the two Bennett 4R mechanisms. Therefore, the order of the twist system composed of the twist of all the six joints in the single-loop 6R mechanism is $C = 3 + 3 - 2 = 4$. The basis of the twist system composed of the twist of all the six joints in the single-loop 6R mechanism can

[2] Whether the DOF of a mechanism obtained using this formula or alike is of full-cycle (or finite motion) should be detected using certain procedure such as those for parallel mechanisms [22,25] and for Bennett mechanisms-based single-loop overconstrained mechanisms in this paper. In some literature, the instantaneous DOF were regarded to be of full cycle without any detection. This may lead to wrong results in some cases.

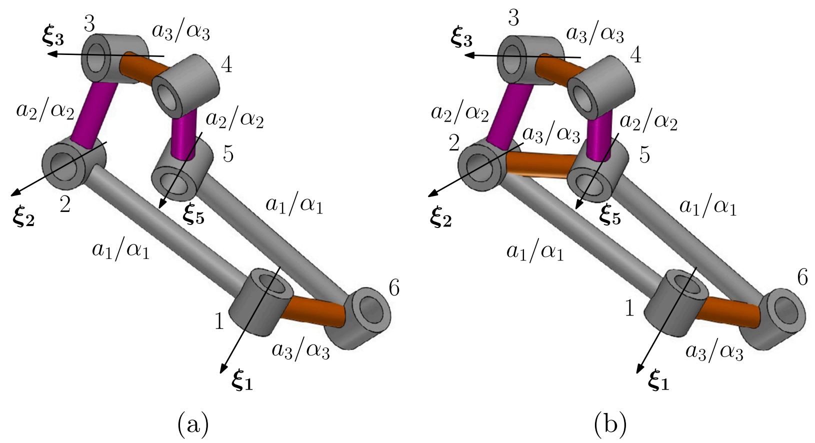

Fig. 4. Mobility analysis of a single-loop spatial mechanism: (a) 2-DOF 6R single-loop mechanism; (b) 2-DOF 2-loop 7-link mechanism.

be represented by (ξ_2, ξ_5, ξ_1 and ξ_3). Using Eq. (2), we obtain the instantaneous DOF of the single-loop 6R mechanism (Fig. 4(a)) as

$$\mathcal{F} = f - C = 6 - 4 = 2 \tag{4}$$

2.2. The approach to the type synthesis

From Eq. (2), it is learned that the value for C of a variable-DOF single-loop mechanism composed of R joints may vary in different motion modes of the mechanism. Since a variable-DOF mechanism may have a non-overconstrained motion mode in which $C = 6$ and an overconstrained motion mode in which $C < 6$, the key to the type synthesis of variable-DOF single-loop mechanisms is the type synthesis of multi-DOF overconstrained single-loop mechanisms composed of no less than seven R joints.

This paper will focus on variable-DOF single-loop mechanisms that can be constructed using Bennett 4R mechanisms (Fig. 2) and Goldberg 5R mechanisms (Fig. 5). As will be shown in Section 3.3, 1-DOF overconstrained 4-link mechanisms composed of R, P and H joints [15] other than the Bennett mechanism are not applicable for constructing variable-DOF single-loop mechanisms. For the construction of variable-DOF single-loop mechanisms involving planar or spherical sub-kinematic chains, please refer to [1,11,12].

The Goldberg 5R mechanism [28] (Fig. 5(a) can be obtained from the 1-DOF 2-loop 6-link overconstrained mechanism shown in Fig. 5(b), which is composed of two Bennett mechanisms 1-2-3-6-1 and 3-4-5-6-3 with a common ternary link 156 and has a 2-DOF multiple joint 3,[3] by removing link 36 and sub-links 16 and 56. In Fig. 5(a) and throughout this paper, two coaxial hollow cylinders in a single-loop mechanism represents an R joint like one hollow cylinder. This extra hollow cylinder is retained to show the trace of construction of the single-loop mechanism.

The links of the Goldberg 5R mechanism can be classified into three groups based on the characteristics of link parameters: links 12 and 45, which have the same link length and twist angle, link 23 with $B_{23} = \pm B_{12}$ and link 34 with $B_{34} = \pm B_{12}$, link 15 the link length and twist angle of which are a function of those of links 23 and 34 and can be determined using the formula of a spatial triangle [21]. The offsets along joints 1 and 5 are not 0 in a general case but could be 0 in a specific case (Fig. 5(c)). Without loss of generality, Goldberg 5R mechanisms with no offset (Fig. 5(c)) will be used for illustrating the construction of multi-loop or variable-DOF single-loop mechanisms for simplicity and clarity reasons.

This class of variable-DOF single-loop spatial mechanisms can be constructed in three steps:

Step 1 To construct multi-DOF multi-loop overconstrained mechanisms using Bennett 4R mechanisms and Goldberg 5R mechanisms.

Step 2 To obtain multi-DOF single-loop overconstrained mechanisms;
Step 3 To construct variable-DOF single-loop spatial mechanisms.

3. Construction of variable-DOF single-loop spatial mechanisms

Using the steps for the type synthesis in Sec 2.2, variable-DOF single-loop spatial mechanisms will be constructed using Bennett 4R mechanisms and Goldberg 5R mechanisms below.

[3] An $\mathcal{F}$-DOF multiple joint allows $(\mathcal{F}+1)$ links to rotate with respect to each other about the same axis.

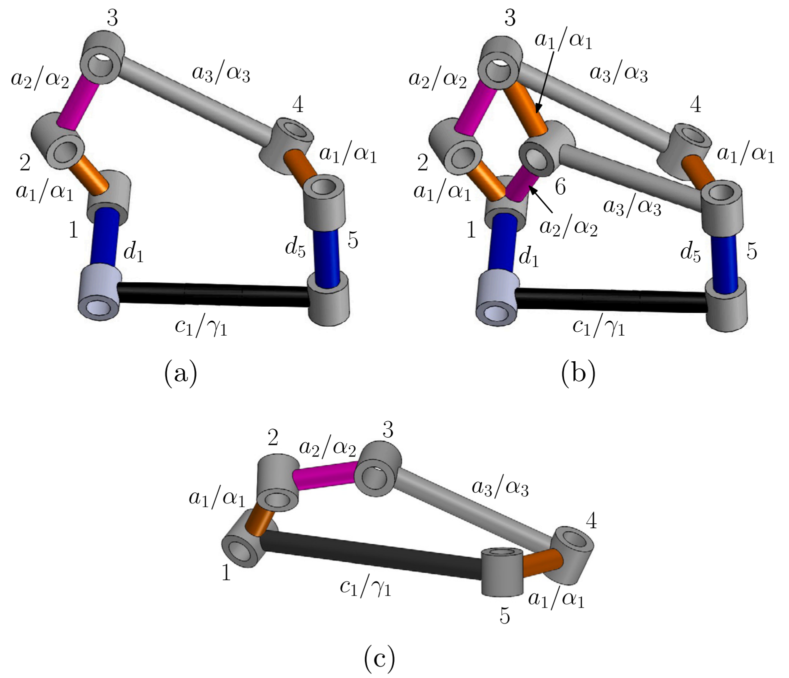

Fig. 5. Goldberg 5R mechanism: (a) General case; (b) Construction of the mechanism; and (c) Case with no offset.

3.1. Step 1: To construct multi-DOF multi-loop overconstrained mechanisms

By adding one or more Bennett 4R mechanisms to a Bennett 4R mechanism or a Goldberg 5R mechanism, we can construct multi-DOF multi-loop overconstrained mechanisms. The addition of a Bennett 4R mechanism to a mechanism needs to meet the following condition: the number of joints/links in the longest-loop of the obtained mechanism is larger than the number of joints/links in the longest-loop of the original mechanism.

For the type synthesis of variable-DOF single-loop mechanisms, we only require $\mathcal{F}(\mathcal{F} > 1)$-DOF multi-loop overconstrained mechanisms in which the number of joints in the longest-loop of the mechanism is less than $(\mathcal{F}+6)$. This ensures that the single-loop mechanism composed of the longest-loop of the mechanism is a multi-DOF single-loop overconstrained mechanism.

Five 2-DOF 2-loop overconstrained mechanisms (Figs. 6 and 7) and three 3-DOF multi-loop overconstrained mechanisms (Fig. 8) have been obtained.

The 2-DOF 2-loop 7-link overconstrained mechanism I in Fig. 6(a) is composed of two Bennett mechanisms 1-2-5-6-1 and 2-3-4-5-2 which have a common link 25. The 2-DOF 2-loop 7-link overconstrained mechanism II in Fig. 6(b) is composed of two Bennett mechanisms 1-2-3-4-1 and 4-5-6-7-4, which have a common ternary link 147. Joints 2 and 5 in mechanism I (Fig. 6(a)) and joint 4 in mechanism II (Fig. 6(b)) are all 2-DOF multiple joint.

Each of the three 2-DOF 2-loop 8-link overconstrained mechanisms in Fig. 7 is composed of a Goldberg 5R mechanism and a Bennett 4R mechanism. Although these mechanisms have the same topological structure, they are of different types due to the characteristics of link parameters presented in Section 2.2 or bond diagram [29] of the generalized Goldberg 5R mechanism. For example, the 2-DOF 2-loop 8-link overconstrained mechanism I in Fig. 7(a) is obtained by adding a Bennett 4R mechanism 3-4-5-6-3 to a Goldberg 5R mechanism 1-2-3-6-7-1 with a common link 36.

The 3-DOF 2-loop 8-link overconstrained mechanism in Fig. 8(a) is composed of two Bennett mechanisms 1-2-3-4-1 and 4-5-6-7-4 in which joint 4 is a 3-DOF multiple joint. The offset between links 34 (or 47) and 45 (or 14) is denoted by d_4'. Similarly, the 3-DOF three-loop 10-link overconstrained mechanisms in Figs. 8(b) and 8(c) are each composed of three Bennett mechanisms.

It is noted that the 2-DOF multi-loop spatial mechanism in Fig. 6(a) was used in the construction of 1-DOF Goldberg overconstrained 5R mechanisms [16,28]. The 3-DOF multi-loop spatial mechanism in Fig. 8(a) and those in Figs. 8(b) and 8(c) were used in the construction of the 1-DOF hybrid overconstrained 6R mechanism in [15] and 1-DOF Goldberg overconstrained 6R mechanisms in [16] respectively.

3.2. Step 2: To obtain multi-DOF single-loop overconstrained mechanisms

From each multi-DOF multi-loop overconstrained mechanism obtained in Step 1, one can readily obtain a multi-DOF single-loop overconstrained mechanism by taking the longest loop of the mechanism. For example (Figs. 6 and 9), from the 2-DOF 2-loop 7-link overconstrained mechanism I (Fig. 6(a)), we can obtain a 2-DOF single-loop 6R mechanism 1-2-3-4-5-6-1 (Fig. 9(a)) by removing

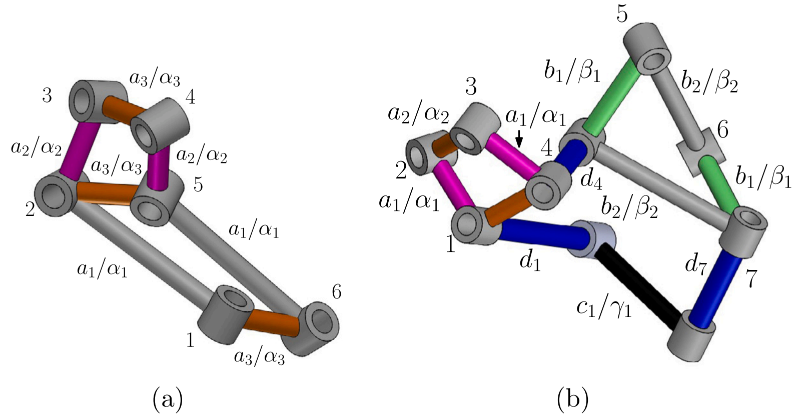

Fig. 6. Construction of 2-DOF 2-loop spatial mechanisms using Bennett mechanisms: (a) 2-loop 7-link mechanism I; (b) 2-loop 7-link mechanism II.

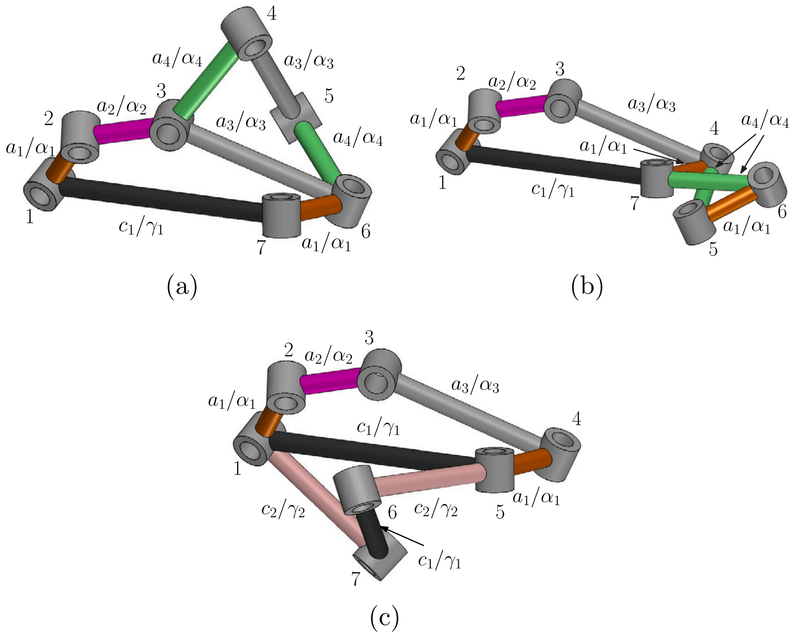

Fig. 7. Construction of 2-DOF 2-loop spatial mechanisms using a Bennett mechanism and a Goldberg 5R mechanism: (a) 2-loop 8-link mechanism I; (b) 2-loop 8-link mechanism II; and (c) 2-loop 8-link mechanism III.

link 25. Multiple joints 2 and 5 in Fig. 6(a) becomes R joints 2 and 5 in Fig. 9(a). In Section 2.1, we have proved that this mechanism has two DOF. Similarly, we can determine the DOF of the single-loop overconstrained mechanisms presented in this section using the approach presented in Section 2.1.

From the 2-DOF 2-loop 7-link overconstrained mechanism II (Fig. 6(b)), we can obtain a 2-DOF single-loop 7R mechanism 1-2-3-4-5-6-7-1 (Fig. 10(a)) by removing sub-links 14 and 47 of the ternary link. Multiple joint 4 in Fig. 6(b) becomes R joint 4 in Fig. 10(a).

From the 2-DOF 2-loop 7-link overconstrained mechanism I (Fig. 7(a)), we can obtain a 2-DOF single-loop 7R mechanism 1-2-3-4-5-6-7-1 (Fig. 11(a)) by removing link 36.

From the 3-DOF 2-loop 8-link overconstrained mechanism I (Fig. 8(a)), we can obtain a 3-DOF single-loop 8R mechanism 1-2-3-4-5-6-7-8-1 (Fig. 12(a)). The multiple joint 4 in Fig. 8(a) becomes R joint 4, which connects links 34 and 45, and R joint 8, which connect links 78 and 81, in Fig. 12(a). In the 3-DOF mode, the axes of R joints 4 and 8 coincide. As will be explained later in Section 3.3, this 8R mechanism also have a 2-DOF mode in which the axes of R joints 4 and 8 generally do not coincide anymore.

Fig. 13(a) shows a 3-DOF single-loop 8R spatial mechanism 1-2-3-4-5-6-7-8-1, which is obtained from the 8R loop of the 3-DOF 3-loop overconstrained mechanism III (Fig. 8(c)) by removing links 14 and 47.

Following the above procedure, one 2-DOF single-loop 6R mechanism (Fig. 9(a)), four 2-DOF single-loop 7R mechanisms (Fig. 14) and three 3-DOF single-loop 8R mechanisms (Fig. 15) have been obtained.

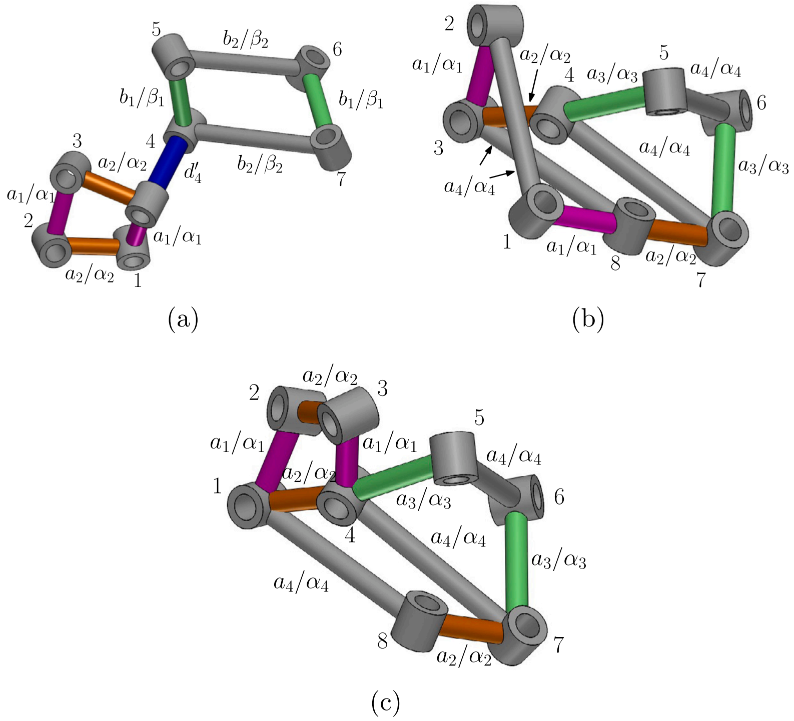

Fig. 8. Construction of 3-DOF multi-loop spatial mechanisms using Bennett mechanisms: (a) 2-loop 8-link mechanism; (b) 3-loop 10-link mechanism I; (c) 3-loop 10-link mechanism II.

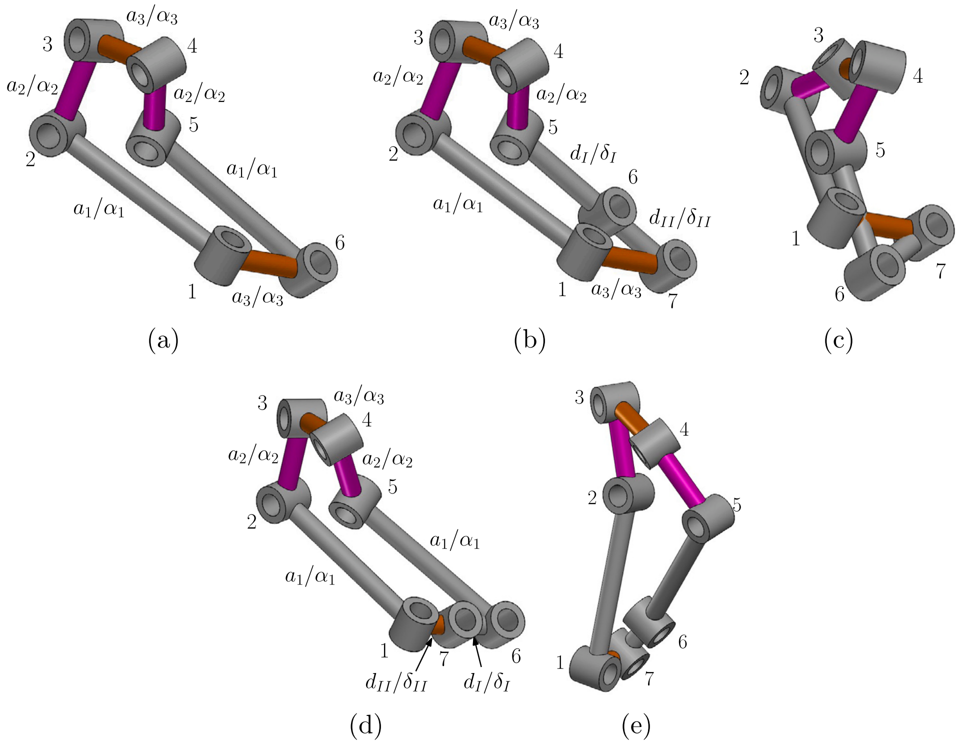

Fig. 9. Construction of variable-DOF single-loop spatial mechanisms from a 2-DOF 2-loop 6-link mechanism shown in Fig. 6(a): (a) 2-DOF 6R single-loop mechanism; (b) Variable-DOF single-loop 7R mechanism I in 2-DOF 6R mode; (c) Variable-DOF single-loop 7R mechanism I in 1-DOF 7R mode; (d) Variable-DOF single-loop 7R mechanism II in 2-DOF 6R mode; (e) Variable-DOF single-loop 7R mechanism II in 1-DOF 7R mode.

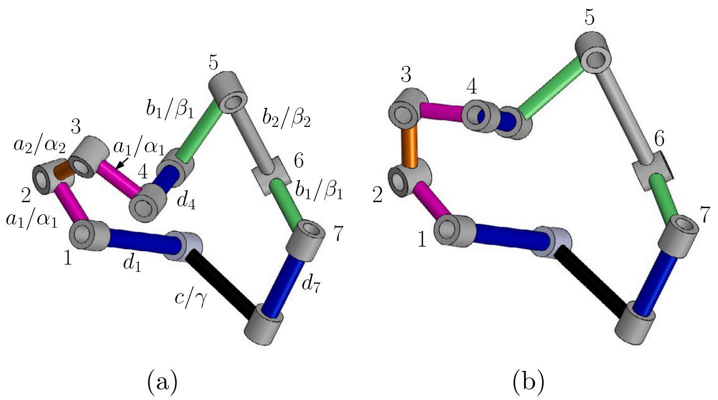

Fig. 10. A variable-DOF single-loop 7R mechanism constructed from the 2-DOF 2-loop mechanism shown in Fig. 6(b) in: (a) 2-DOF 7R mode; (b) 1-DOF 7R mode.

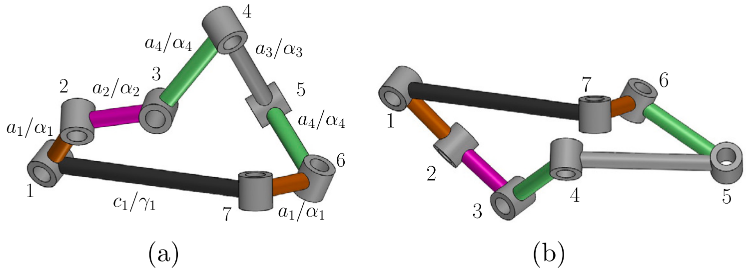

Fig. 11. A variable-DOF single-loop 7R mechanism constructed from the 2-DOF 2-loop mechanism shown in Fig. 7(a) in: (a) 2-DOF 7R mode; (b) 1-DOF 7R mode.

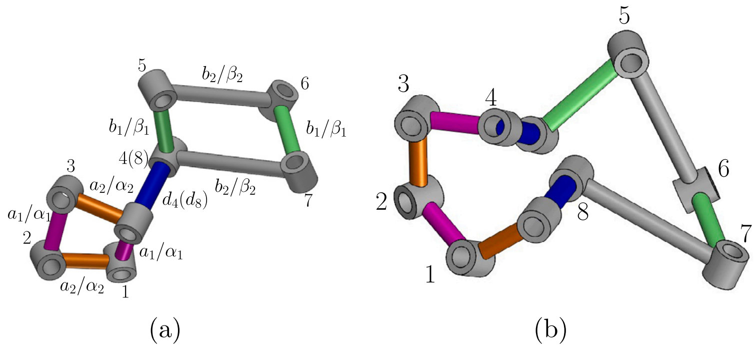

Fig. 12. A variable-DOF single-loop 8R mechanism 1-2-3-4-5-6-7-8-1 constructed from the 3-DOF 2-loop mechanism shown in Fig. 8(a) in: (a) 3-DOF 8R mode; (b) 2-DOF 8R mode.

3.3. Step 3: To construct variable-DOF single-loop mechanisms

From the 2-DOF single-loop 6R overconstrained mechanism (Fig. 9(a)) obtained in Step 2, one can construct two types of variable-DOF single-loop 7R mechanisms (Figs. 9(b)–9(c) and 9(d)–9(e)) by inserting an R joint to the 6R mechanism. Using the approach to the mobility analysis of single-loop mechanisms (Section 2.1), we can prove that these single-loop 7R mechanisms have a 2-DOF motion mode. On one hand, the DOF of each of these single-loop 7R mechanisms is not less than 2 (the DOF of the original single-loop 6R mechanism in Fig. 9(a)). On the other hand, the twist system composed of the twist of all the seven joints in the single-loop 7R mechanism is equal to 5 (the sum of 4 (the order of the twist system composed of the twist of the six joints in the original 6R mechanism) and 1 (the order of the twist system of the inserted R joint), and the instantaneous DOF of each single-loop 7R mechanism (Figs. 9(b) and 9(d)) can be calculated using Eq. (2) as

$$\mathcal{F} = f - C = 7 - 5 = 2 \tag{5}$$

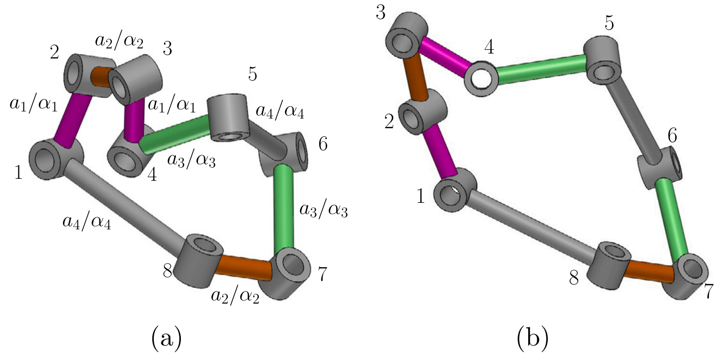

Fig. 13. A variable-DOF single-loop 8R mechanism constructed from the 3-DOF 3-loop mechanism shown in Fig. 8(c) in: (a) 3-DOF 8R mode; (b) 2-DOF 8R mode.

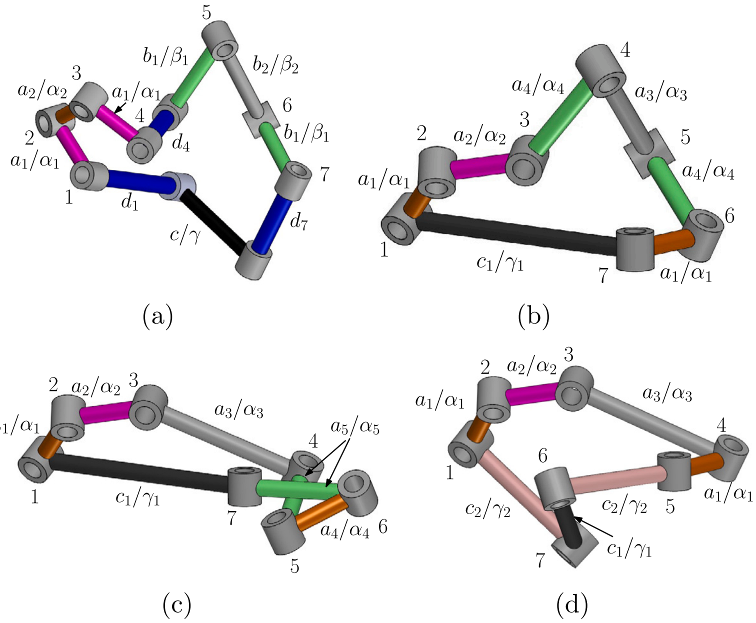

Fig. 14. 2-DOF single-loop 7R mechanisms.

In the 2-DOF motion mode, the inserted R joint of each 7R mechanism loses its DOF (Figs. 9(b) and 9(d)) [22], and the mechanism works like the original single-loop 6R mechanism.

The construction of the above two single-loop 7R mechanisms, as well as the other 2-DOF single-loop 7R and all the 3-DOF single-loop 8R overconstrained mechanisms described in Section 3.2, shows that at least six links in each single-loop 7R mechanism, and all the links in each single-loop 8R mechanism, have two skew joint axes. Consequently, all of these single-loop mechanisms must also have a non-overconstrained motion mode and are thus variable-DOF mechanisms.

For example, in addition to the 2-DOF overconstrained motion mode (Figs. 9(b) and 9(d)), the above two single-loop 7R mechanisms also have a 1-DOF single-loop 7R non-overconstrained motion mode (Figs. 9(c) and 9(e)).

The single-loop 7R mechanism in Fig. 10 has a 2-DOF motion mode (Fig. 10(a)) and a non-overconstrained 1-DOF motion mode (Fig. 10(b)). In addition to the 2-DOF 7R motion mode (Fig. 11(a)), the single-loop 7R mechanism in Fig. 11 also has a 1-DOF 7R non-overconstrained motion mode (Fig. 11(b)).

The single-loop 8R mechanism in Fig. 12 has a 3-DOF motion mode (Fig. 12(a)), in which the axes of R joints 4 and 8 usually coincide, and a 2-DOF non-overconstrained motion mode (Fig. 12(b)), in which the axes of R joints 4 and 8 usually do not coincide. In addition to its 3-DOF 8R motion mode (Fig. 13(a)), the single-loop 8R mechanism in Fig. 13 also has a 2-DOF non-overconstrained 8R motion mode (Fig. 13(b)).

Following the above procedure, six variable-DOF single-loop 7R mechanisms (Table 1) and three variable-DOF single-loop 8R mechanisms (Table 2) have been constructed using Bennett 4R mechanisms and Goldberg 5R mechanisms.

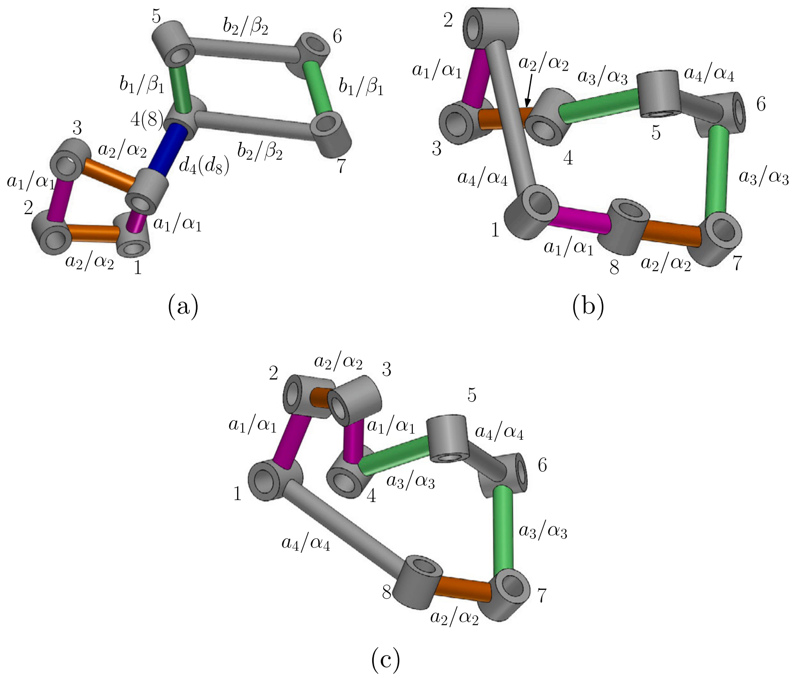

Fig. 15. 3-DOF single-loop 8R mechanisms.

No variable-DOF single-loop mechanisms can be constructed from 1-DOF overconstrained 4-link mechanisms composed of R, P and H joints [15] other than the Bennett mechanism by using the above procedure. This is due to the requirements that a common binary link should be shared between two compositional overconstrained 4-link mechanisms in the construction of multi-DOF multi-loop overconstrained mechanisms (see Fig. 8(b) for example) and that the resulted single-loop mechanism should be able to reach a non-overconstrained motion mode with $C = 6$. For example, it would be impossible for a planar 4R and a Bennett mechanism to share a common binary link. The single-loop mechanism obtained from the 3-DOF 2-loop mechanism composed of a planar 4R mechanism and a spherical 4R mechanism in the same topology as the one shown in Fig. 8(a) cannot reach a non-overconstrained motion mode with $C = 6$ [22].

Isomeric variations of the above variable-DOF mechanisms can be obtained by isomerization [30]. Let a Bennett dyad [31] be two links connected by an R joint with the same absolute value of Bennett ratio and zero joint offset. For example, one Bennett dyad in Bennett 4R mechanism 1-2-3-4-1 (Fig. 2) is Bennett dyad 1-2-3. If two Bennett dyads can constitute a Bennett 4R kinematic chain (Bennett dyads 1-2-3 and 3-4-1), one Bennett dyad is referred to as the complement Bennett dyad of the other. Isomerization of a single-loop mechanism refers to replacing a Bennett dyad of the mechanism with its complement Bennett dyad (Fig. 16). Figs. 16(a)–16(c) show three of the isometric variations, which are all variable-DOF 8R mechanisms, obtained from the variable-DOF 8R mechanism shown in Fig. 16(d) by isomerization. Isomeric variation I in Fig. 16(a) is obtained from the variable-DOF 8R mechanism (Fig. 16(d)) by replacing Bennett dyad 8-1-2 with its complement Bennett dyad 8-1'-2 (Fig. 16(e)). Please note the Bennett dyad to be replaced should not belong to the same compositional Bennett 4R mechanism (Fig. 16(f)) of the original single-loop mechanism. Similarly, Isomeric variation II in Fig. 16(b) is obtained from the variable-DOF 8R mechanism (Fig. 16(d)) by replacing Bennett dyad 3-4-5 with its complement Bennett dyad 3-4'-5, while Isomeric variation III in Fig. 16(c) is obtained from Isomeric variation I (Fig. 16(a)) by replacing Bennett dyad 1'-2-3 with its complement Bennett dyad 1'-2'-3.

In an $\mathcal{F}$-DOF motion mode, a variable-DOF mechanism will be turned into a structure if $\mathcal{F}$ joints are locked. Using a CAD software, we can obtain the DOF of a mechanism by locking its joints one by one until the mechanism is reduced to a structure. We have verified that all the above variable-DOF single loop 7R mechanisms have both a 1-DOF motion mode and a 2-DOF motion mode, and all the above variable-DOF single loop 8R mechanisms have both a 2-DOF motion mode and a 3-DOF motion mode.

Except the No. 3 variable-DOF single-loop 7R mechanism in Table 1 and the No. 1 variable-DOF single-loop 8R mechanism in Table 2 which have been presented in [2,5,8,13], the remaining variable-DOF single-loop mechanisms proposed in this paper are new. A special case of the No. 1 variable-DOF single-loop 8R mechanism in Table 2 was also proposed in [32] for constructing a deployable polyhedron but it was not realized to be a variable-DOF mechanism since this 8R mechanism cannot reach a 3-DOF mode during the motion of the deployable polyhedrons. The 8R mechanism shown in Fig. 16(b) has been used in the construction of overconstrained 6R mechanisms [33,34] and reconfiguration between different overconstrained 6R mechanisms [35], but it was thought to be a 3-DOF single-loop overconstrained mechanism instead of a variable-DOF mechanism as described in this paper.

The reconfiguration analysis of the No. 3 variable-DOF single-loop 7R mechanism [2,14] has shown that this single-loop 7R mechanism has a 1-DOF 7R mode and a 2-DOF 7R mode. All the transition configurations in which the 7R mechanism can transit

Table 1
Six variable-DOF single-loop 7R mechanisms.

<table>
<tr><th>No</th><th>2-DOF motion mode</th><th>1-DOF motion mode</th><th>Description</th></tr>
<tr><td>1</td><td>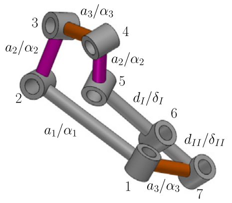</td><td>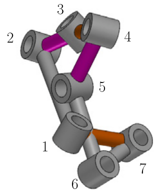</td><td>$\begin{cases} L_{71} = L_{34} \\ \alpha_{71} = \alpha_{34} \\ L_{23} = L_{45} \\ \alpha_{23} = \alpha_{45} \\ B_{12} = \pm B_{23} = \pm B_{71} \\ d_i = 0 \quad i = 1,2,3 \textit{ and } 4 \end{cases}$
L_{56}, L_{67}, α_{56}, α_{67}, d_5, d_6, and d_7 are functions of L_{12} and α_{12}.</td></tr>
<tr><td>2</td><td>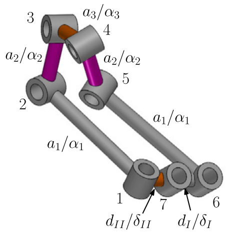</td><td>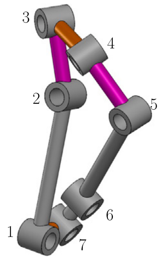</td><td>$\begin{cases} L_{12} = L_{56} \\ \alpha_{12} = \alpha_{56} \\ L_{23} = L_{45} \\ \alpha_{23} = \alpha_{45} \\ B_{12} = \pm B_{23} = \pm B_{34} \\ d_i = 0 \quad i = 2,3,4 \textit{ and } 5 \end{cases}$
L_{67}, L_{71}, α_{67}, α_{71}, d_1, d_6, and d_7 are functions of L_{34} and α_{34}.</td></tr>
<tr><td>3</td><td>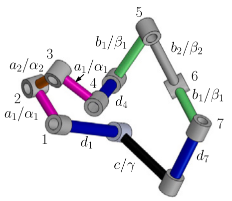</td><td>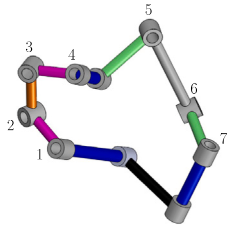</td><td>$\begin{cases} L_{12} = L_{34} \\ \alpha_{12} = \alpha_{34} \\ L_{67} = L_{45} \\ \alpha_{67} = \alpha_{45} \\ B_{12} = \pm B_{23} \\ B_{45} = \pm B_{56} \\ d_i = 0 \quad \text{i=2, 3, 5 and 6} \end{cases}$
L_{71}, α_{71}, d_1, and d_7 are functions of L_{23}, L_{56}, α_{23}, α_{56}, and d_4.</td></tr>
<tr><td>4</td><td>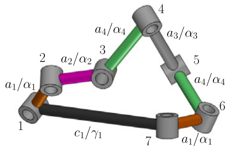</td><td>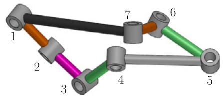</td><td>$\begin{cases} L_{12} = L_{67} \\ \alpha_{12} = \alpha_{67} \\ L_{34} = L_{56} \\ \alpha_{34} = \alpha_{56} \\ B_{12} = \pm B_{23} = \pm B_{34} = \pm B_{45} \\ d_i = 0 \quad i = 2,3,\dots,6 \end{cases}$
L_{71}, α_{71}, d_1, and d_7 are functions of L_{23}, L_{45}, α_{23}, and α_{45}.</td></tr>
<tr><td>5</td><td>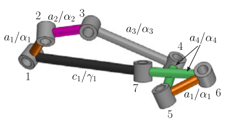</td><td>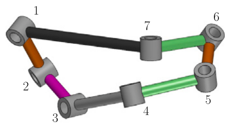</td><td>$\begin{cases} L_{12} = L_{56} \\ \alpha_{12} = \alpha_{56} \\ L_{45} = L_{67} \\ \alpha_{45} = \alpha_{67} \\ B_{12} = \pm B_{23} = \pm B_{34} = \pm B_{45} \\ d_i = 0 \quad i = 2,3,\dots,6 \end{cases}$
L_{71}, α_{71}, d_1, and d_7 are functions of L_{23}, L_{34}, α_{23}, and α_{34}.</td></tr>
<tr><td>6</td><td>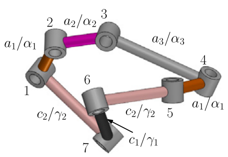</td><td>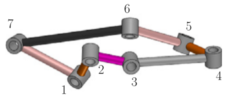</td><td>$\begin{cases} L_{12} = L_{45} \\ \alpha_{12} = \alpha_{45} \\ L_{56} = L_{71} \\ \alpha_{56} = \alpha_{71} \\ B_{12} = \pm B_{23} = \pm B_{34} = \pm B_{45} \\ B_{56} = \pm B_{67} \\ d_i = 0 \quad i = 2,3,4,6,7 \end{cases}$
L_{67}, α_{67}, d_1, and d_5 are functions of L_{23}, L_{34}, α_{23}, and α_{34}.</td></tr>
</table>

between different motion modes have also been identified. In a transition configuration of a variable-DOF single-loop 7R mechanism, the value for C is 4 [1,2], and the instantaneous DOF of the mechanism is 3 (=7-4). In [36], all the 2-DOF and 3-DOF 8R motion modes of a specific case of the No. 1 variable-DOF single-loop 8R mechanism have been identified. It is noted that the geometric characteristics of a transition configuration of a variable-DOF mechanism, such as the transition configuration with 3 instantaneous DOF (Fig. 17) of the variable-DOF mechanism shown in Fig. 10, may not be as apparent as those in [1,2,36]. The reconfiguration analysis of the remaining variable-DOF single-loop 8R mechanisms and their isometric variations deserve further investigation.

Table 2
Three variable-DOF single-loop 8R mechanisms.

No	3-DOF motion mode	2-DOF motion mode	Description
1	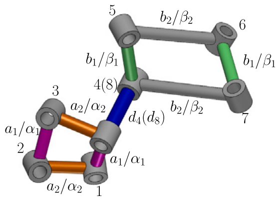	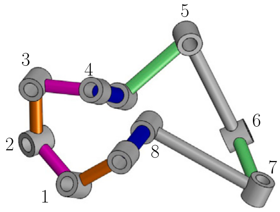	$\left\{\begin{array}{l} L_{81} = L_{23} \\ \alpha_{81} = \alpha_{23} \\ L_{12} = L_{34} \\ \alpha_{12} = \alpha_{34} \\ L_{45} = L_{67} \\ \alpha_{45} = \alpha_{67} \\ L_{56} = L_{78} \\ \alpha_{56} = \alpha_{78} \\ B_{81} = \pm B_{12} \\ B_{45} = \pm B_{56} \\ d_i = 0 \quad i = 1,2,3,5,6,7 \\ d_8 = d_4 \end{array}\right.$
2	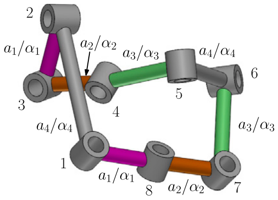	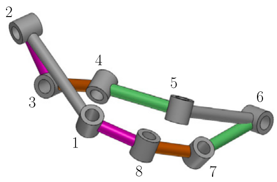	$\left\{\begin{array}{l} L_{81} = L_{23} \\ \alpha_{81} = \alpha_{23} \\ L_{12} = L_{56} \\ \alpha_{12} = \alpha_{56} \\ L_{45} = L_{67} \\ \alpha_{45} = \alpha_{67} \\ L_{34} = L_{78} \\ \alpha_{34} = \alpha_{78} \\ B_{81} = \pm B_{12} = \pm B_{34} = \pm B_{45} \\ d_i = 0 \quad i = 1,2,\ldots,8 \end{array}\right.$
3	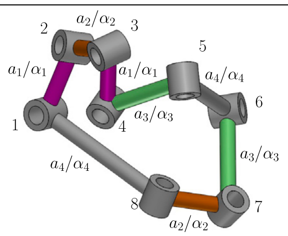	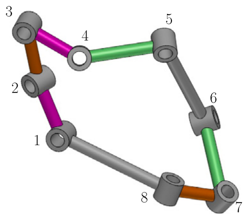	$\left\{\begin{array}{l} L_{81} = L_{56} \\ \alpha_{81} = \alpha_{56} \\ L_{12} = L_{34} \\ \alpha_{12} = \alpha_{34} \\ L_{45} = L_{67} \\ \alpha_{45} = \alpha_{67} \\ L_{23} = L_{78} \\ \alpha_{23} = \alpha_{78} \\ B_{81} = \pm B_{12} = \pm B_{23} = \pm B_{45} \\ d_i = 0 \quad i = 1,2,\ldots,8 \end{array}\right.$

It has been proved in [37] that every $(n-5)$-DOF nR linkage with $n > 6$ “has parallel neighboring axes or triples of consecutive axes that satisfy a Bennett condition”. The work in this paper shows that there is probably no $(n-5)$-DOF nR linkage with only triples of consecutive axes that satisfy a Bennett condition if $n > 8$. Whether this statement is true remains to be investigated.

4. Conclusions

A construction approach to the type synthesis of variable-DOF single-loop mechanisms using Bennett 4R mechanisms and Goldberg 5R mechanisms has been proposed. All the existing Bennett-4R-mechanism-based variable-DOF single-loop 7R and 8R spatial mechanisms in the literature have been obtained along with five new variable-DOF single-loop 7R spatial mechanisms, two new variable-DOF single-loop 8R spatial mechanisms and their isomeric variations.

This paper, together with [1], provides a systematic construction approach to the type synthesis of variable-DOF single-loop spatial mechanisms. This work enriches the types of variable-DOF single-loop spatial mechanisms and provides a solid foundation for further research on variable-DOF single-loop spatial mechanisms. The application of variable-DOF single-loop mechanisms as potential adaptive fixtures in reconfigurable manufacturing systems should be explored. Whether there exist variable-DOF nR ($n > 8$) mechanisms with only triples of consecutive axes that satisfy a Bennett condition also deserves investigation using the approach presented in [14,37,38].

Declaration of competing interest

The authors declare that they have no known competing financial interests or personal relationships that could have appeared to influence the work reported in this paper.

Acknowledgments

This work was supported by the Engineering and Physical Sciences Research Council [EP/T024844/1], United Kingdom.

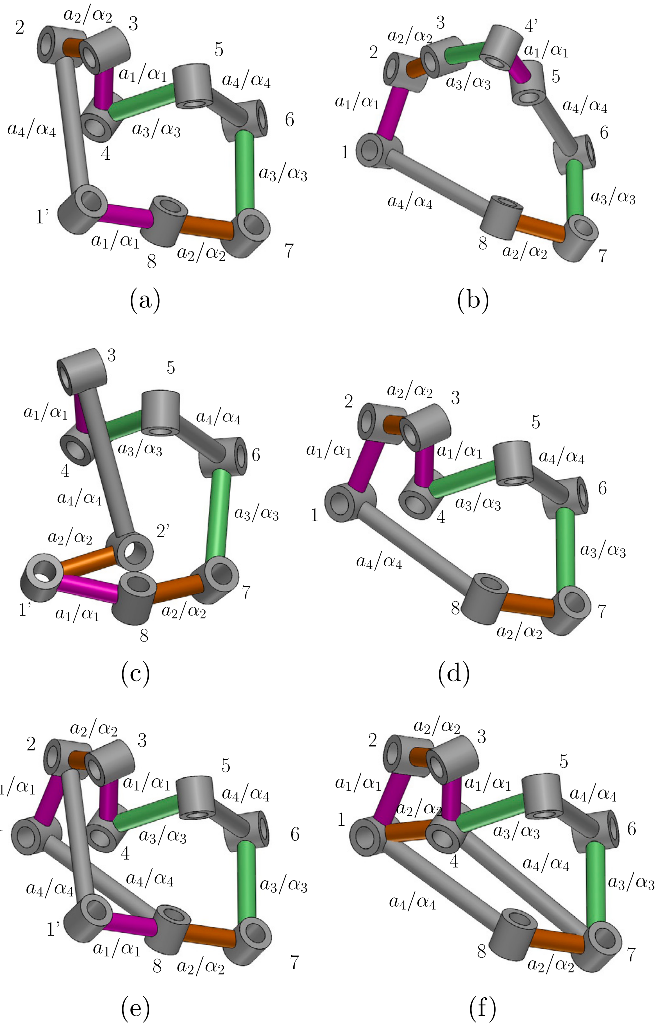

Fig. 16. Three isometric variations of variable-DOF 8R mechanisms via isomerization in 3-DOF mode: (a) Isomeric variation I; (b) Isomeric variation II; (c) Isomeric variation III; (d–f) Isomerization for obtaining Variation I.

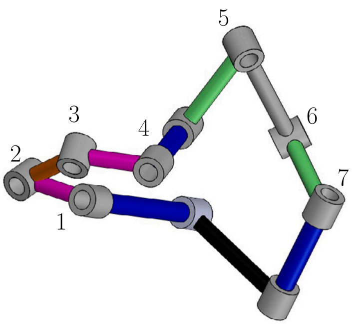

Fig. 17. A transition configuration of the variable-DOF single-loop 7R mechanism shown in Fig. 10.

Data availability

No data was used for the research described in the article.

References

[1] X. Kong, M. Pfurner, Type synthesis and reconfiguration analysis of a class of variable-DOF single-loop mechanisms, Mech. Mach. Theory 85 (2015) 116–128.
[2] M. Pfurner, X. Kong, Algebraic analysis of a new variable-DOF 7R mechanism, in: New Trends in Mechanism and Machine Science: Theory and Industrial Applications, Springer, 2016, pp. 71–79.
[3] C. Galletti, P. Fanghella, Single-loop kinematotropic mechanisms, Mech. Mach. Theory 36 (6) (2001) 743–761.
[4] K. Wohlhart, Kinematotropic linkages, in: Recent Advances in Robot Kinematics, Springer, 1996, pp. 359–368.
[5] R. Wang, Y. Song, J.S. Dai, Reconfigurability of the origami-inspired integrated 8r kinematotropic metamorphic mechanism and its evolved 6R and 4R mechanisms, Mech. Mach. Theory 161 (2021) 104245.
[6] C.R. Díez-Martínez, Mobility and Connectivity in Spatial Kinematic Chains, Technological Institute of Celaya, Celaya, Mexico, 2005 (in Spanish).
[7] H. Feng, Y. Chen, J.S. Dai, G. Gogu, Kinematic study of the general plane-symmetric bricard linkage and its bifurcation variations, Mech. Mach. Theory 116 (2017) 89–104.
[8] K. Liu, J. Yu, X. Kong, Synthesis of multi-mode single-loop Bennett-based mechanisms using factorization of motion polynomials, Mech. Mach. Theory 155 (2021) 104110.
[9] X. He, X. Kong, D. Chablat, S. Caro, G. Hao, Kinematic analysis of a single-loop reconfigurable 7R mechanism with multiple operation modes, Robotica 32 (7) (2014) 1171–1188.
[10] P. López-Custodio, J. Rico, J. Cervantes-Sánchez, G. Pérez-Soto, Reconfigurable mechanisms from the intersection of surfaces, J. Mech. Robotics 8 (2) (2016) 021029.
[11] M. Ruggiu, X. Kong, Reconfiguration analysis of an RRRRS single-loop mechanism, Robotics 7 (3) (2018) 51.
[12] X. Kong, A variable-DOF single-loop 7R spatial mechanism with five motion modes, Mech. Mach. Theory 120 (2018) 239–249.
[13] X. Chai, C. Zhang, J.S. Dai, A single-loop 8R linkage with plane-symmetry and bifurcation property, in: 2018 International Conference on Reconfigurable Mechanisms and Robots, ReMAR, IEEE, 2018, pp. 1–8.
[14] K. Liu, J. Yu, X. Kong, Structure synthesis and reconfiguration analysis of variable-degree-of-freedom single-loop mechanisms with prismatic joints using dual quaternions, J. Mech. Robotics 14 (2) (2022) 021009.
[15] K.J. Waldron, Hybrid overconstrained linkages, J. Mech. 3 (2) (1968) 73–78.
[16] M. Goldberg, New five-bar and six-bar linkages in three dimensions, Trans. Am. Soc. Mech. Eng. 65 (6) (1943) 649–656.
[17] X. Kong, C. Huang, Type synthesis of single-DOF single-loop mechanisms with two operation modes, in: 2009 ASME/IFToMM International Conference on Reconfigurable Mechanisms and Robots, IEEE, 2009, pp. 136–141.
[18] J. Wang, G. Bai, X. Kong, Single-loop foldable 8R mechanisms with multiple modes, in: New Trends in Mechanism and Machine Science: Theory and Industrial Applications, Springer, 2017, pp. 503–510.
[19] C.-H. Kuo, J.-W. Su, Configuration analysis of a class of reconfigurable cube mechanisms: Mobility and configuration isomorphism, Mech. Mach. Theory 107 (2017) 369–383.
[20] H. Lipkin, A note on denavit-hartenberg notation in robotics, in: International Design Engineering Technical Conferences and Computers and Information in Engineering Conference, Vol. 47446, 2005, pp. 921–926.
[21] C. Mavroidis, B. Roth, On the geometry of spatial polygons and screw polygons, ASME J. Mech. Des. 119 (2) (1997) 246–252.
[22] X. Kong, C. Gosselin, Type Synthesis of Parallel Mechanisms, Springer, Netherlands, 2007.
[23] G. Gogu, Mobility of mechanisms: a critical review, Mech. Mach. Theory 40 (9) (2005) 1068–1097.
[24] J.S. Dai, Z. Huang, H. Lipkin, Mobility of overconstrained parallel mechanisms, ASME J. Mech. Des. 128 (1) (2006) 220–229.
[25] J.M. Rico, L.D. Aguilera, J. Gallardo, R. Rodriguez, H. Orozco, J.M. Barrera, A more general mobility criterion for parallel platforms, ASME J. Mech. Des. 128 (1) (2005) 207–219.
[26] Z. Huang, J. Liu, D. Zeng, A general methodology for mobility analysis of mechanisms based on constraint screw theory, Sci. China Ser. E: Technol. Sci. 52 (5) (2009) 1337–1347.
[27] T.-L. Yang, D.-J. Sun, A general degree of freedom formula for parallel mechanisms and multiloop spatial mechanisms, J. Mech. Robotics 4 (1) (2012) 011001.
[28] C. Song, Y. Chen, A spatial 6R linkage derived from subtractive goldberg 5R linkages, Mech. Mach. theory 46 (8) (2011) 1097–1106.
[29] G. Hegedüs, J. Schicho, H.-P. Schröcker, Bond theory and closed 5R linkages, in: Latest Advances in Robot Kinematics, Springer, 2012, pp. 221–228.
[30] K. Wohlhart, On isomeric overconstrained space mechanisms, in: Proc. 8th Wld Congr, Vol. 1, IFToMM, Prague, 1991, 1991, pp. 153–158.
[31] J.E. Baker, Screw replacements in isomeric variants of Bricard's line-symmetric six-bar, Proc. Inst. Mech. Eng. C 223 (10) (2009) 2391–2398.
[32] J. Wang, X. Kong, A novel method for constructing multimode deployable polyhedron mechanisms using symmetric spatial compositional units, J. Mech. Robotics 11 (2) (2019) 020907.
[33] K. Wohlhart, Merging two general Goldberg 5R linkages to obtain a new 6R space mechanism, Mech. Mach. Theory 26 (7) (1991) 659–668.
[34] X. Kong, X. He, D. Li, A double-faced 6R single-loop overconstrained spatial mechanism, J. Mech. Robotics 10 (3) (2018) 031013.
[35] C.-Y. Song, H. Feng, Y. Chen, I.-M. Chen, R. Kang, Reconfigurable mechanism generated from the network of Bennett linkages, Mech. Mach. Theory 88 (2015) 49–62.
[36] X. Kong, Motion mode analysis of a variable-DOF 8R spatial mechanism composed of four plane symmetric RRR triads, in: 2024 6th International Conference on Reconfigurable Mechanisms and Robots, IEEE, 2024, pp. 513–518.
[37] T. Duarte Guerreiro, Z. Li, J. Schicho, Classification of higher mobility closed-loop linkages, Ann. Mat. Pura Appl. 202 (2) (2023) 737–762.
[38] J. Frischauf, M. Pfurner, D.F. Scharler, H.-P. Schröcker, A multi-Bennett 8R mechanism obtained from factorization of bivariate motion polynomials, Mech. Mach. Theory 180 (2023) 105143.